Available online at www.sciencedirect.com
ScienceDirect
Journal of the European Ceramic Society 29 (2009) 2481–2489
www.elsevier.com/locate/jeurceramsoc

Friction and wear mechanisms of K_2O–B_2O_3–Al_2O_3–SiO_2–MgO–F glass-ceramics

Atiar Rahaman Molla [a,b], B.V. Manoj Kumar [b], Bikramjit Basu [b,*]

[a] Glass Division, Central Glass and Ceramic Research Institute, Council of Scientific and Industrial Research (CSIR), 196, Raja S.C. Mullick Road, Kolkata 700032, India
[b] Department of Materials and Metallurgical Engineering, Indian Institute of Technology Kanpur, IIT Kanpur 208016, India

Received 11 September 2008; received in revised form 14 February 2009; accepted 3 March 2009
Available online 3 April 2009

Abstract

Among various brittle materials, the mica-based glass-ceramics are of greater scientific interest, because of their machinability. Considering the potential of these materials as dental implants, an understanding of the wear behavior in oral environment is important. In the present investigation, K_2O–B_2O_3–Al_2O_3–SiO_2–MgO–F glass-ceramics containing about 70% crystals, heat treated at 1040 °C for 12 h was subjected to fretting against steel ball in artificial saliva (AS) environment. In order to elucidate the influence of environment on the friction and wear behavior, control experiments were also performed under dry ambient conditions. A systematic decrease in wear rate with test duration was recorded with a minimum wear rate of 10^{-5} mm^3/Nm after 100,000 fretting cycles in AS medium. Scanning electron microscope–energy dispersive spectroscopy (SEM–EDS) analysis indicated the formation and brittle fracture of tribochemical layer in AS medium, whereas mica crystal pull-out was a dominant mechanism in dry conditions.

Keywords: Glass-ceramics; Wear; Artificial saliva

1. Introduction

In last two decades, various biocompatible ceramic and glass-ceramic (GC) materials have been researched for biomedical and dental applications[1]. The dental ceramics/GC are particularly considered for use as restorative materials and supporting structures. Based on the increasing clinical problems associated with the long time wear of the dentine, Mair and others attempted to investigate the wear mechanisms of human teeth and glass-ceramic materials.[2–5] While considerable work has been carried out in microstructural evolution of various GC materials,[6–12] systematic research in understanding the dominant wear mechanisms is rather limited for this important class of material.

In a study on the dry unlubricated sliding behavior, Park and Ozturk[13] demonstrated the dominating influence of the amount and orientation of wollastonite phase on the hardness and wear of the apatite–wollastanite (A–W) GC. The wear resistance of the material decreased as the wollastonite amount is decreased. In different work Xiao et al. observed that the frictional properties of CaO–MgO–Al_2O_3–SiO_2 (CMAS) glass-ceramics were related to the contact pressure and sliding speed, while plastic deformation and recrystallization were identified as dominant wear mechanisms during sliding tests in dry conditions.[14] The tribological study with Dicor glass-ceramic against alumina revealed higher COF of 0.8 in dry conditions.[15] Based on the Hertzian contact studies, it was argued that the wear of mica-containing Macor GC is controlled by the short-crack toughness as well as by the size and volume fraction of mica plates.[15,16]

In a tribological study of feldspathic porcelain ceramics against silicon nitride in simulated oral conditions, Yu et al. illustrated the prominent effect of load than sliding speed and frequency of oscillation.[17] The reduction in friction and wear of cordierite GC was attributed to the formation of thin gel-like reaction layers as a result of ion-exchange in hydrochloric acid, while the network dissolution process was responsible for the increased wear and friction in caustic soda solutions.[18]

* Corresponding author. Tel.: +91 512 2597771, fax: +91 512 2597505x259007.
E-mail address: bikram@iitk.ac.in (B. Basu).

0955-2219/$ – see front matter © 2009 Elsevier Ltd. All rights reserved.
doi:10.1016/j.jeurceramsoc.2009.03.001

Table 1
Composition of base glass used in the present work.

Starting materials	Precursor constituent	Amount (in wt.%)
Quartz powder	SiO_2	48.94
Aluminum nitrate nona hydrate	Al_2O_3	16.29
Magnesium hydroxide carbonate	MgO	17.45
Potassium nitrate	K_2O	7.15
Boric acid (H_3BO_3)	B_2O_3	5.25
MgF_2	F^-	3.85

Nagarajan et al. reported a clear transition of wear from localized fracture at low load to contact or spallation mode at high loads, when mica-containing GC were slided against alumina under distilled water lubrication. It was further argued that microcrack-induced fracture occurs either along the interface of weak mica–glass interface or mica cleavage planes.[19] In another study of the sliding of glass composites against alumina in distilled water, it was found that the wear dominates by formation and delamination/dissolution of the tribochemical layer/products.[20]

The present work is a part of our ongoing research activity in the area of GCs. In our recent work,[21,22] the development of some unusual spherulitic–dendritic crystals as well as their in vitro dissolution properties of K_2O–B_2O_3–Al_2O_3–SiO_2–MgO–F glass-ceramics were reported. In a follow-up work, it was demonstrated how the variation in fluorine content over 1–4% influences the crystallization as well as microstructure development and mechanical properties (hardness, strength) in K_2O–B_2O_3–Al_2O_3–SiO_2–MgO–F glass-ceramics.[23] In particular, these GC materials exhibited higher hardness and comparable elastic modulus values than that observed in any other dental restorative materials.[21] In order to explore the potential of this compositionally varied GC system for use as dental restorative material, a clear understanding of the tribological behavior is essential. In this perspective, the purpose of the present work is to understand the friction and wear behavior of the K_2O–B_2O_3–Al_2O_3–SiO_2–MgO–F glass-ceramic material with 70% mica crystal content, when subjected to fretting against steel. A major part of the work is focused in elucidating the influence of environment on the mechanisms of material removal, when tested in dry and AS medium.

2. Experimental procedure

2.1. Production and characterization of GC

The composition used for production of GC in the K_2O–B_2O_3–Al_2O_3–SiO_2–MgO–F system is given in Table 1. Various precursor materials used to produce the base glass include high purity optical grade quartz flour (Sipur A1 Bremthaler Quartzitwerk, Germany), aluminum nitrate nona hydrate (Riedel-de-Hahn AG, Germany), magnesium hydroxide carbonate (Merck, Germany), potassium nitrate (Merck, Germany), boric acid (Merck KGaA, Germany), and MgF_2 (Merck KGaA, Germany). The glass batch of appropriate composition was mixed by Eirich Mixer (Germany) for 5 min, and thereafter, melting of the glass composition was carried out in a platinum crucible at 1550 °C for 2 h using electrical furnace. The glass melts were cast into a mild steel mould to obtain plates, and subsequent annealing was performed for 2 h in the temperature range of 600–650 °C. The composition of the base glass was analyzed by inductively coupled plasma atomic emission spectroscopy (ICP-AES) (spectroflame modula FTM 08, Germany). Two-stage heat-treatment was done to crystallize the glass to convert into GC. The nucleation was done in the temperature range of 750–850 °C for 6 h, followed by crystallization at 1040 °C for 12 h holding time. Our earlier study[23] illustrated that the combination of the above processing scheme produces glass-ceramic material with optimal combination of crystal volume fraction and mechanical properties. The heating and cooling rates were maintained at 180 °C/h throughout the heat treatment cycle. The surfaces of the samples were polished using standard metallographic (emery) papers and finally with diamond paste (from 9 to 0.25 μm). The final surface roughness of the samples prior to wear testing was measured using Laser surface profilometer (PGK-120, Mahr, Germany) and found in the order of 0.05 μm. The spatial resolution and vertical resolution of the profilometer are 0.1 μm and 0.5 nm, respectively (claimed by the manufacturer). The polished surface was etched with 12% hydrofluoric acid (HF) with varying time of 1–3 min at different zones of the sample for revealing the crystal morphology in the bulk GC sample. The conventional point counting method using SEM images of the etched surfaces revealed a large amount (70 vol.%) of mica crystals in the investigated GC material. Various mechanical properties of the GC material are listed in Table 2. More details about the properties of the GC can be found in our recent paper.[23]

Table 2
Mechanical and physical properties of the glass ceramic (GC), used in the tribological study.

Density (gm/cc)	2.83
Three-point flexural strength (MPa)	80.6 ± 7.7
Elastic modulus (GPa)	69.7 ± 2.9
Vickers hardness (GPa)	6.4 ± 1.2

2.2. Tribological study

The tribological experiments were performed using a computer-controlled fretting machine (DUCOM TR281-M, Bangalore, India), which produces linear relative oscillating motion with ball-on-flat configuration. By a stepper motor, the flat sample was made to oscillate with a relative linear displacement of constant stroke and frequency. The displacement of the flat sample was monitored by an inductive displacement transducer and a piezoelectric transducer was used to measure the friction force. Variation in tangential force was recorded and the corresponding COF was calculated on-line with the help of a computer-based data acquisition system. More details of the tribometer can be found elsewhere.[24] Polished GC bars

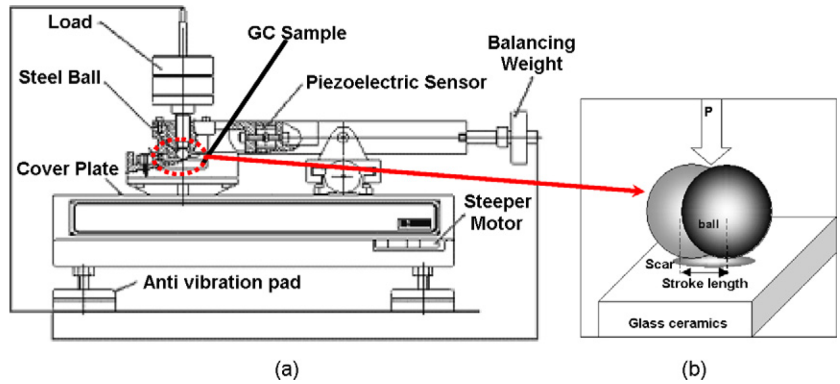

Fig. 1. (a) Schematic diagram of the fretting wear tester and (b) tribological contact. P is applied load.

of 25 mm × 5 mm × 4 mm were used as flat (moving) materials and commercial SAE 52100-grade steel (hardness ∼ 7 GPa) balls of 10 mm diameter were selected as counterbody (stationary) materials. It can be noted here that the ideal mating material would have been natural human tooth. However, steel counterbody was chosen based on two reasons: (a) similar hardness as that of the developed GC or dental prosthetic materials (Ni–Cr alloy, ceramic, etc.) and (b) the difficulties in preparation of ball samples with human tooth material. Similar wear studies of dental materials against steel were also previously reported.[25] Schematic of the selected tribological contact is shown in Fig. 1(b). Prior to wear testing, both GC and steel samples were ultrasonically cleaned using acetone. The fretting tests were carried out in ambient conditions in air without using any lubricant (dry conditions), and using AS medium with selected parameters of 1 N load, 8 Hz oscillation frequency and 100 μm (gross slip regime) linear stroke length. The composition of AS is given in Table 3. The experiments were done for different test durations of 5000, 10,000, 50,000 and 100,000 cycles.

After wear testing, the surfaces were cleaned with acetone and the wear volume was computed from the measured transverse wear scar diameter using Klaffke's equation.[26] It must be noted that the use of this equation is justified for fretting conditions where the wear scar diameter is larger than twice the Hertzian contact diameter, which is in accordance with our experiments. Furthermore, from the estimated wear volumes, the wear rates [wear volume/load × sliding distance) mm^3/Nm] were calculated. SEM–EDS analysis was performed in order to identify the dominant mechanisms of material removal.

Table 3
Composition of artificial saliva.

Material	Amount (gm) per 1 L of distilled water	Comment
NaCl	0.4	99.9% pure, AR grade
KCl	0.4	99.5% pure, AR grade
$CaCl_2 \cdot 2H_2O$	0.795	99.5% pure, AR grade
$NaH_2PO_4 \cdot 2H_2O$	0.78	99% pure, AR grade
$Na_2S \cdot 9H_2O$	0.005	99.9% pure, AR grade
Urea	1	99.5% pure, AR grade

3. Results

3.1. Friction and wear data

The friction and wear properties of investigated GC against steel were evaluated both in air (dry) and AS media for different test durations. The COF was measured continuously during the entire test period. All the tests were repeated for two to three times and the reproducibility of the frictional behavior is fairly confirmed. In Fig. 2, the average value of experimentally measured COF is plotted against test duration for GC/steel tribocouples in both conditions of dry and AS. In general, COF sharply increases within first few thousand cycles and thereafter attains the steady state condition. A higher COF value of 0.88 was recorded for the GC/steel couple when tests were conducted in dry conditions, while a COF of 0.67 was recorded in case of AS medium tests. Also, noticeable fluctuations still appear throughout the steady state region for both the cases.

The high COF value measured in dry conditions can be attributed either due to the interaction of the asperities of two mating surfaces or due to the interaction of glass-ceramic asperity with hard debris particles. As will be mentioned below,

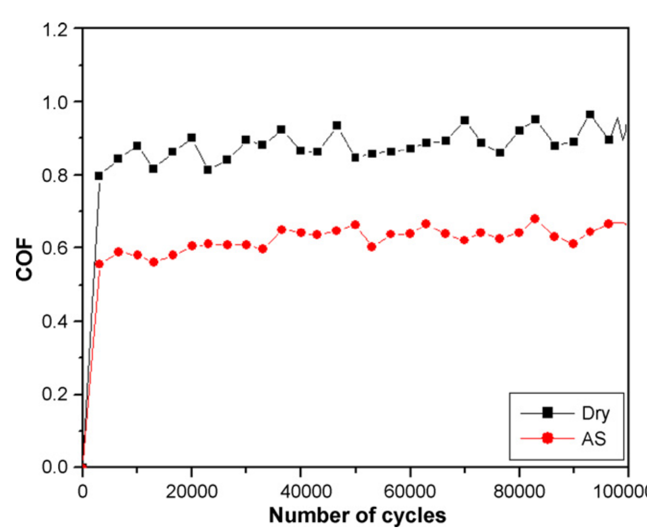

Fig. 2. Evolution of COF during fretting of investigated GC in dry and AS environment. Counter body: 10 mm diameter steel ball; load: 1 N; stroke length: 100 μm; oscillation frequency: 8 Hz.

the wear involving steel counterbody always produces iron oxide debris particles, which are even harder than steel mating body. Therefore, the abrasion by hard oxide debris in case of dry conditions, i.e. more contributions from the second factor will evidently lead to increased COF. However, such scenario changes in AS medium and the particular effect of AS medium on the friction and wear behavior will be further discussed in a later section.

The wear rate data for the investigated GC materials is presented in Fig. 3. Irrespective of environment, the wear rate systematically decreases with the fretting test duration. It appears that the wear rate for the investigated GCs in the selected tribological environment varies in the range of 10^{-4} to 10^{-5} mm^3/Nm. Considering the application of extremely low load (1 N) and also low sliding velocity (much less than 0.1 m/s), the wear rate of the investigated GC against steel is one order of magnitude higher than that of various structural ceramic materials (typical wear rate ~10^{-6} mm^3/Nm), investigated earlier in our group.[27] Such difference is obvious to expect because of much lower hardness of the presently investigated GC materials. However, when compared with other GC materials, the wear rate of the investigated GC is at least one order of magnitude lower.[15] Further, it is evident from Fig. 3 that wear rate is less in AS medium than in dry conditions at any given test duration. The wear rate decreases systematically from 3.5×10^{-4} to 1.2×10^{-5} mm^3/Nm during fretting of GC in dry or AS environment. After fretting for 100,000 cycles, a maximum wear rate of 9×10^{-5} mm^3/Nm is measured for GC in dry conditions, while a minimum wear rate of 1×10^{-5} mm^3/Nm for GC in AS medium. From the above observation of lower magnitude of wear rate and decreasing trend in wear rate with test duration, longer durabil-

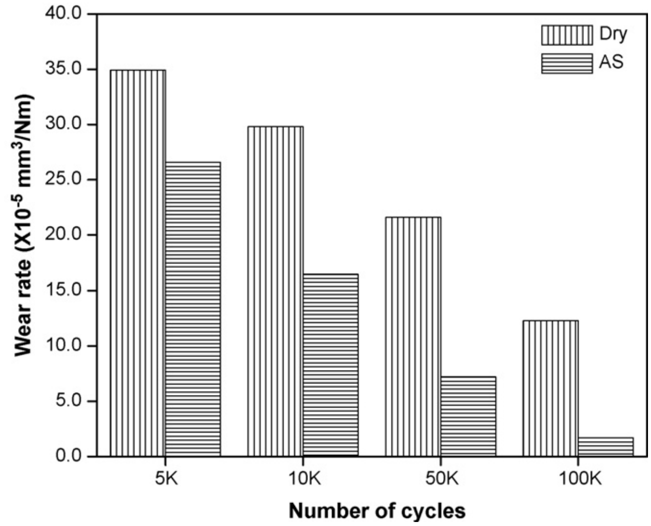

Fig. 3. Wear rate of GC after fretting in dry and AS medium for different time duration. Around 10–15% deviation around the reported data were measured in our experimental results.

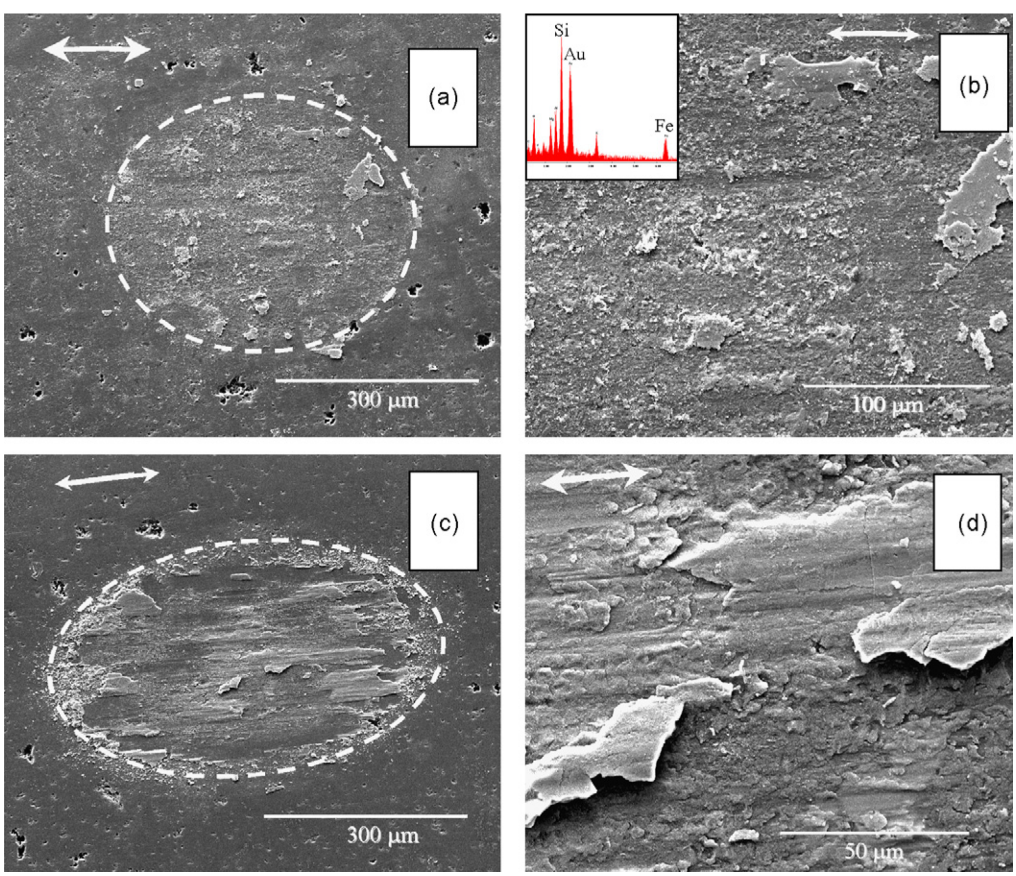

Fig. 4. SEM image illustrating the overall fretting damage experienced by GC plate, after testing against steel ball at 1 N load for 5000 cycles, 8 Hz frequency, 100 µm stroke length (a and b) in dry condition and (c and d) AS medium. Inset in (b) shows EDS analysis of the corresponding worn surface. The doubly pointed arrows indicate fretting directions.

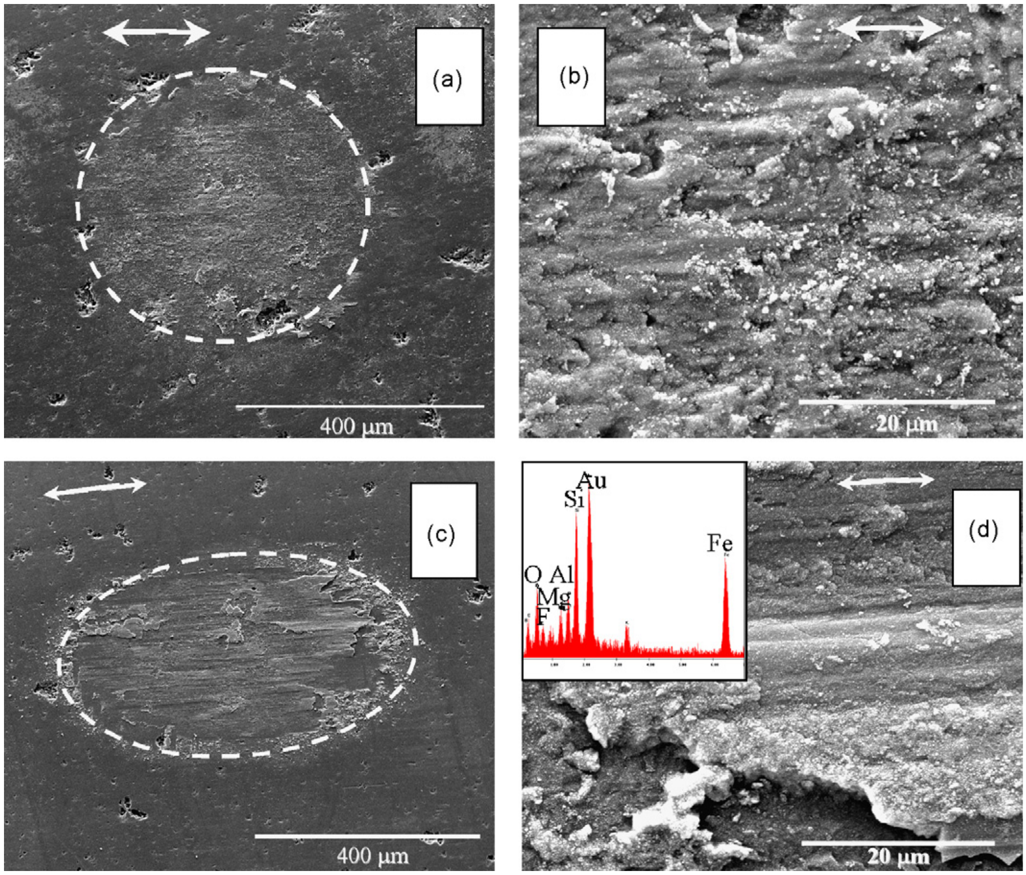

Fig. 5. SEM image illustrating the fretting damage experienced by GC plate, after testing against steel ball in dry condition (a and b) and AS (c and d) at 1 N load for 10,000 cycles, 8 Hz frequency, 100 μm stroke length. Inset in (d) shows EDS analysis of the tribolayer. The doubly pointed arrows indicate fretting directions.

ity or better wear resistance during long-term application of the presently investigated GC could be expected.

3.2. Wear mechanisms

In order to understand the nature of dominant mechanisms during the wear process, detailed SEM–EDS analysis of worn surfaces of investigated GC samples was conducted after fretting against steel in different environment. Some representative SEM images of the worn surfaces at different stages (number of cycles) of fretting are presented in Figs. 4 through 7.

During initial stages, the overall fretting damage of the GC in dry conditions reveals dispersion of small size debris particles (Fig. 4a and b). EDS analysis (inset in Fig. 4b) reveals the presence of iron along with the glass elements (aluminium, magnesium, silicon, fluorine, potassium, oxygen, etc.), indicating material transfer from steel ball. However, the tribolayer formation is significantly absent in dry conditions. On the other hand, the worn surface is mainly characterized by the formation of tribolayer after fretting in AS medium for 5k cycles (Fig. 4c and d). Though the layer does not cover entire area of the wear scar, deformation or smearing of the smooth layer is certainly evident. Fig. 5 represents the worn surfaces of GC after 10k cycles. The striking difference from the earlier stage is the severity of the wear in terms of considerable pull-outs and increased number of debris when fretted in dry conditions (Fig. 5b). However, the absence of potential tribolayer indicates that its formation is not feasible after 10k cycles. In case of AS medium, a thick tribolayer appears to form, while its removal is evident through peel-off or delamination (Fig. 5d). Further, one may note that the wear scar is elliptical, when compared against circular wear scar in dry conditions (Fig. 5c).

The roughness, pull-outs as well as the number of agglomerated brighter debris particles increased, when the wear progresses to 50k cycles in dry conditions. When the EDS spectrum of the unworn GC surface (inset in Fig. 6a) is compared with that of debris (inset in Fig. 6b), it can be understood that fretting results in the pull-out, and oxidation of the constituents of GC as well as the counterbody steel material. Further, the iron found in the debris on the worn surface of GC indicates material transfer from steel ball. On the other hand, prolonged duration of fretting in AS medium resulted in the small and elliptical wear scar that is completely covered with the dense layer (Fig. 6c). The dispersion of debris around the periphery of the wear scar is interesting to note, which is otherwise absent in case of dry conditions. Such dispersion of debris might be attributed to the continuous flushing in and out of the AS due to the reciprocating action of fretting. High magnification SEM image of the GC worn surface after 50k fretting cycles (Fig. 6d) reveals the presence of large number of cracks, indicating the characteristic brittle fracture and spalling of the tribolayer. Similar features were explained as a result of contact fracture and

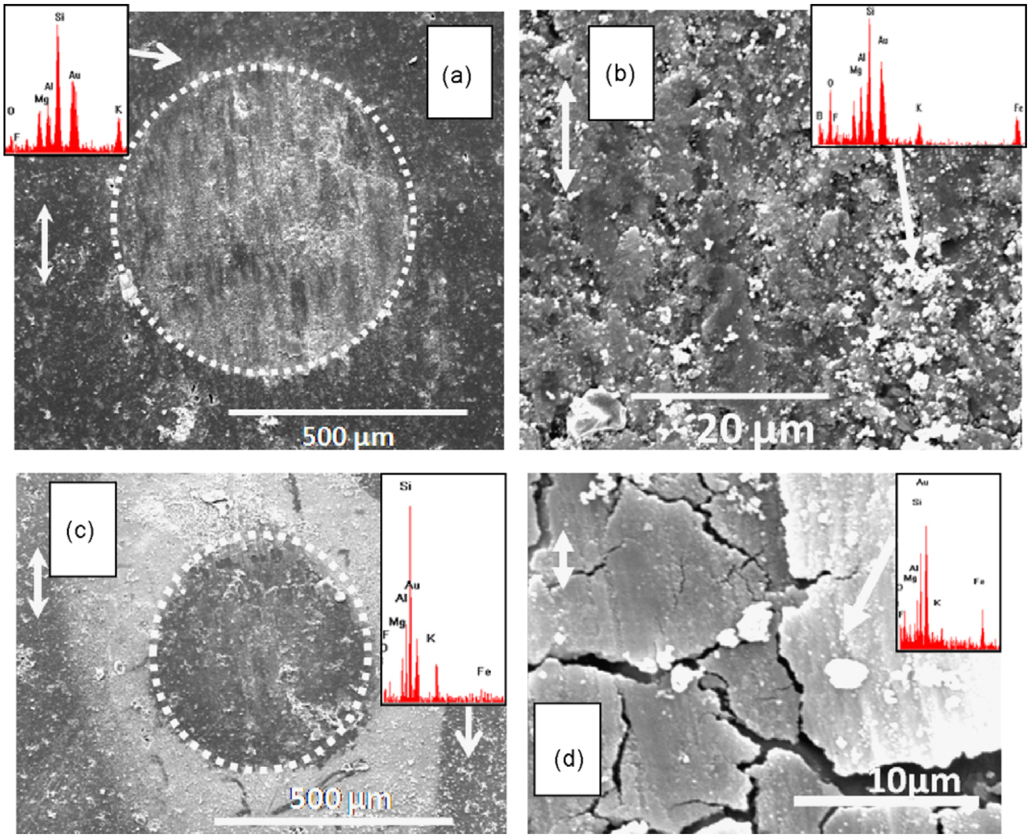

Fig. 6. SEM image illustrating the overall fretting damage experienced by GC plate, after testing against steel ball at 1 N load for 50,000 cycles, 8 Hz frequency, 100 µm stroke length in (a and b) dry and (c and d) AS medium. EDS analysis of the respective unworn surfaces are shown as insets (a) and (c), while that of worn surfaces are provided as insets (b) and (d). The doubly pointed arrows indicate fretting directions.

spalling, when Dicor GC was slided against alumina in distilled water environment.[19] The opening-up of cracks indicates the hygroscopic nature of the layers, formed during fretting in AS medium.

The severity of the pull-outs is further increased with increase in number of cycles (100k) in dry conditions (Fig. 7). Further, Fig. 7b reveals the formation of thin layer fragments and their smearing on the worn surface after 100k cycles. The characteristics of the worn surface after 100k cycles in AS medium are, in general, similar to that after 50k cycles, namely the elliptical and smaller wear scar, formation of potential tribolayer protecting the base surface, the dispersion of fine debris around the periphery of the wear scar and the brittle nature of the tribolayer with number of cracks. In addition, the tribochemical layer is observed to have fine grooves in the fretting direction, indicating mild abrasion due to the sliding of hard debris particles (see Fig. 7d).

4. Discussion

Based on the above mentioned observations of friction, wear and topographical features of the worn surfaces, the influence of the AS medium on the fretting wear behavior of the investigated GC during fretting against steel can be discussed.

As the hardness difference between the mating materials is minimal, the local welding and detachment of asperity junctions result in the significant adhesion during initial stages of fretting in dry conditions. The steep raise of the COF plot during running-in-period could be attributed to this fact. During progress of the fretting, asperities are subjected to deformation or fracture, resulting in the formation of debris. The interaction of the either surfaces with continuously evolving debris, provide steady state in the frictional behavior. The debris are transferred to the counter surface and/or subjected to oxidation in ambient conditions of testing. Further, the hard debris particles are responsible for abrading the counter surface. Thus, the debris consists oxides of both the mating surfaces (see EDS analysis).

The hard oxide debris formed during continuous fretting results in the three-body wear. In dry conditions, the prolonged fretting results in the formation of increased number of agglomerated debris. Further, the higher value of average COF value ($\sim$0.9) observed throughout the test duration necessarily indicates that the wear occurs mainly through the removal of crystalline mica phase (Fig. 2). When tests were conducted in AS medium, it is highly possible that the pulled-out mica debris particles are subjected for the hydroxylation. This could be noted as significant effect of corrosion phenomenon occurring at the wet tribocontacts.[28] The hydroxides are eventually compacted to form tribochemical layer during extended fretting such that it protects the base GC surface from further wear. The decreased friction/wear rate against that in dry conditions is in agreement with this fact. The presence of macrocracks on the tribochemical

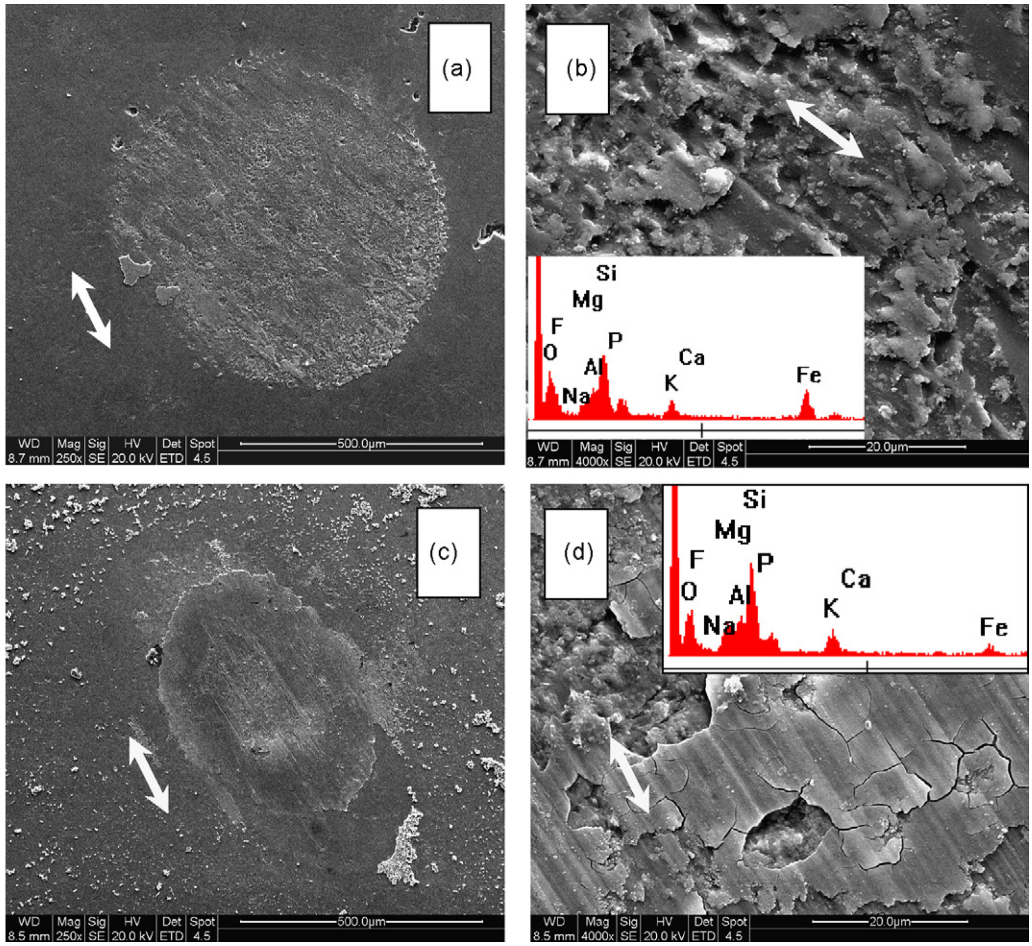

Fig. 7. SEM image illustrating the overall fretting damage experienced by GC plate, after testing against steel ball at 1 N load for 100,000 cycles, 8 Hz frequency, 100 μm stroke length in (a and b) dry and (c and d) AS medium. Insets in (b) and (d) reveal EDS spectra of the worn surface after fretting in dry and AS medium, respectively. The doubly pointed arrows indicate fretting directions.

layer suggests drying of the viscous layer, resulting in the brittle fracture.

In order to analyze the thermo-mechanical effect at the dry tribocontact, we have analytically computed both Hertzian contact stress as well the maximum contact temperature rise. Following Hertzian contact mechanics approach,[29] the initial contact pressure is calculated as 196 MPa and the initial contact diameter is ∼40 μm. Observing Figs. 4–7, it is clear that the fretting at the tribocontact considerably expand the scar diameter to 500–600 μm, depending on the number of testing cycles. Such a considerable increase in scar diameter reduces the contact pressure to 0.51–0.35 MPa. In addition, the Archard's model[30] estimated very low rise in contact temperature (17 °C) at the dry tribocontact in the present case. Such negligible contact temperature rise should be attributed to the combination of low load (1 N) and sliding speed (0.0016 m/s). From the above, it is therefore clear that the extent of wear damage must be related to the contact stress severity, than to the thermal effect when tests were conducted in dry conditions. Further, worn surfaces in dry conditions reveal rough surfaces than that in AS medium. The contrast in the back-scattered electron (BSE) images indicates that the crystalline glass phase is pulled-out during the wear. Considering the large amount (70%) of mica crystalline phase in the unworn GC, its easy pull-out from the soft glass phase and subsequent fracture is highly possible during fretting process.

On the other hand, the evolution of hydroxide-rich tribolayer is responsible for the reduction in wear rate in AS medium. The failure of the layer and the fracture of crystalline phases resulted in the higher COF value (∼0.67); however less than that observed in dry conditions. Therefore, it is understood from the above observation that the dominant wear mechanism changes from stress-induced mechanical wear at dry contact to the corrosion-induced tribochemical wear at wet contacts, when GC is fretted against steel.

The implication of the present investigation is significant in terms of the influence of the saliva on the wear performance of the developed dental restorative GC material. In dry conditions, the COF and wear are high due to the mica crystals pull-outs and abrasion. On the other hand, the presence of AS medium is beneficial in reducing the friction and wear by forming dense viscous tribochemical layer. Based on the present experimental results obtained under the selected fretting conditions and also in the backdrop of the good combination with the in vitro reactivity,[23] the investigated mica-based GC materials appear to be a better choice for use in dental applications.

Table 4
Summary of the tribology test results obtained with some of earlier developed GCs as well as human teeth and comparison with the presently investigated GC. The variation in friction/wear rate depends on the variation in operating conditions.

Tribocouple	Operating conditions	COF	Wear rate (mm^3/Nm)	Wear mechanisms	Reference
Human teeth vs. steel	20 N, dry/AS, 0.002 m/s	0.8–1.2 (dry) 1.0 (AS)	–	Oxidative wear and microfracture	25
Human teeth vs. Al_2O_3	1 N, AS, 0.0005 m/s, 8000 cycles	0.12–0.55	–	Fretting fatigue; adhesive wear	5
Dicor vs. Al_2O_3	4.9 N, 0.0014 m/s, dry	0.7–0.077	2.6×10^{-3}	Microfracture	15
Dicor vs. Al_2O_3	1 N, 0.0025 m/s, distilled water	0.4–0.6	10^{-3} to 10^{-4}	Localized fracture	19
$CaO–MgO–Al_2O_3–SiO_2$ (self-mated)	0.01–0.5 m/s, dry, contact pressure 0.1–1.4 MPa	0.05–0.65	10^{-3} to 10^{-4}	Microcracking, abrasion	14
$MgO–CaO–SiO_2–P_2O_5–F$ vs. ZrO_2	10 N, 0.025 m/s, dry	0.75	0.7×10^{-4}	Abrasive and adhesive wear	13
$K_2O–B_2O_3–Al_2O_3–SiO_2–MgO–F$ vs. steel	1 N, 0.0016 m/s, dry/AS, 100,000 cycles	0.88 (dry); 0.67 (AS)	12×10^{-5} (dry); 2×10^{-5} (AS)	Tribomechanical wear (dry); tribochemical wear (AS)	Present work

Finally, it is instructive to compare the tribological properties of the presently investigated GC material with that of the earlier developed material. In an effort to do so, a summary of the friction and wear rate data along with the operating parameters for some of the earlier developed GCs and commercial Dicor materials is provided in Table 4. In addition, some results of the test with human teeth are also mentioned in Table 4. It is known that the Dicor material, developed commercially for dental restorative applications, exhibit a modest combination of hardness (350 MPa), E-modulus (66.2–91.1 GPa) and strength property (127 MPa). A comparison of presently developed material with Dicor and our material, in terms of tribological properties, indicate a better wear resistance property and comparable frictional property in artificial saliva under similar operating condition (see Table 4). It is therefore likely that the present GC material will have better durability than Dicor. As far as the frictional properties of human teeth are concerned, the presently investigated GC material/steel couple has lower COF than human teeth/steel mating couple. Also, our material exhibits comparable tribological properties like $MgO–CaO–SiO_2–P_2O_5–F/ZrO_2$ tribocouple. As far as the mechanisms of material removal are concerned, Table 4 indicates that the microfracture/tribomechanical wear is the major wear mechanisms for the GC. While this is true in dry conditions for the present case, this paper also adds that the tribochemical layer formation governs wear in AS medium.

At the close, a comprehensive comparison in terms of mechanical and wear properties of the presently investigated GC with that of the earlier developed GCs indicate good potential as dental restorative material (also see Ref. 23). However, further work is needed to assess the optical translucency, machinability and long term durability property. The preliminary work in our laboratory reveals the good biological compatibility, in terms of good cell viability (MTT tests) of human osteoblast cells as well as better anti-microbial property (*E. coli* and *S. epidermidis* cell line) of the presently investigated GC system. However, *in vivo* osseointegration (clinical trials) needs to be carried out before their applications can be realized.

5. Conclusions

A glass-ceramic with 70% mica crystals in $K_2O–B_2O_3–Al_2O_3–SiO_2–MgO–F$ system was heat treated at 1040 °C for 12 h and subjected to fretting wear against steel in dry and AS environments. The initial Hertzian contact stress was 196 MPa for the selected operating parameters. The influence of the environment and fretting duration on the friction and wear behavior of GC material can be summarized as follows:

(a) The co-efficient of friction increased during initial running-in-period and thereafter, attained steady state period, irrespective of the fretting environment. However, a higher value of steady state COF ~ 0.88 was measured at dry contact, while in AS medium, much lower COF 0.67 was recorded. A higher COF in ambient condition commensurate well with the severity in abrasion.
(b) Wear rate varied in the order of 10^{-4} to 10^{-5} mm^3/Nm and a systematic decrease in wear rate with test duration was recorded in both cases of testing medium. A comparison with the earlier developed GC as well as commercial Dicor material reveals better combination of the friction and wear resistance property of the investigated glass-ceramic.
(c) The topographical observations of the worn surfaces using SEM–EDS analysis indicate that the material was removed primarily by tribomechanical wear assisted by pull out of crystals in dry conditions, whereas the formation and brittle fracture of tribochemical layer was dominant in AS medium. In addition, the material transfer from the counterbody was also observed in both ambient environment and AS medium.
(d) Irrespective of the test environment, large amount of debris particles are formed and found to be dispersed largely around wear scars. In AS medium, the stability of the thick tribochemical layer appears to govern the material removal. The occasional spalling of the tribolayer contributes to wear, but to a lower extent than that in dry/ambient conditions.

References

1. Sulong, M. Z. A. M. and Aziz, R. A., Wear of materials used in dentistry: a review of the literature. *Journal of Prosthetic Dentistry*, 1990, **63**, 342–349.
2. Jones, D. W., Jones, P. A. and Wilson, H. J., A simple abrasion test for composites. *Dental Materials*, 1972, **1**, 28–34.
3. Mair, L. H., Wear in dentistry–current terminology. *Journal of Dentistry*, 1992, **20**, 140–144.
4. Mair, L. H., Stolarskij, T. A., Vowles, R. W. and Lloyd, C. H., Wear mechanisms, manifestations and measurement; Report of a workshop. *Journal of Dentistry*, 1996, **24**, 141–148.
5. Roy, S. and Basu, B., Mechanical and tribological characterization of human tooth. *Materials Characterization*, 2008, **59**, 747–756.
6. Gebhardt, A., Höche, T., Carl, G. and Khodos, I. I., TEM study on the origin of cabbage-shaped mica crystal aggregates in machinable glass-ceramics. *Acta Materialia*, 1999, **47**, 4427–4434.
7. Höche, T., Habelitz, S. and Khodos, I. I., Origin of unusual fluorophlogopite morphology in mica glass-ceramics of the system SiO_2–Al_2O_3–MgO–K_2O–Na_2O–F_2. *Journal of Crystal Growth*, 1998, **192**, 185–195.
8. Radonji, L. J., Radonjic, L. J. and Nikoli, The effect of fluorine source and concentration on the crystallization of machinable glass-ceramics. *Journal of the European Ceramic Society*, 1991, **7**, 11–16.
9. Cheng, K., Wan, J. and Liang, K., Crystallization of R_2O–MgO–Al_2O_3–B_2O_3–SiO_2–F ($R = K^+$, Na^+) glasses with different fluorine source. *Materials Letters*, 2001, **47**, 1–6.
10. Clausbruch, S. C. V., Schweiger, M., Höland, W., Rheinberger, V., The effect of P_2O_5 on the crystallization and microstructure of glass ceramics in the SiO_2–Li_2O–K_2O–ZnO–P_2O_5 system. Journal of Non-Crystalline Solids, 2000, 263 & 264, 388-394.
11. Habelitz, S., Höche, T., Hergt, R., Carl, G. and Rüssel, C., Microstructural design through epitaxial growth in extruded mica glass-ceramics. *Acta Materialia*, 1999, **47**, 2831–2840.
12. Höche, T., Habelitz, S. and Avramov, I., Crystal morphology engineering in SiO_2–Al_2O_3–MgO–K_2O–Na_2O–F^- mica glass-ceramics. *Acta Materialia*, 1999, **47**, 735–744.
13. Park, J. and Ozturk, A., Tribological properties of MgO–CaO–SiO_2–P_2O_5–F^- based glass-ceramic for dental applications. *Materials Letters*, 2007, **61**, 1916–1921.
14. Xiao, H., Cheng, Y., Yang, Q. and Senda, T., Mechanical and tribological properties of calcia–magnesia–alumina–silica-based glass-ceramics prepared by in situ crystallization. *Materials Science and Engineering A*, 2006, **423**, 170–174.
15. Jahanmir, S. and Dong, X., Wear mechanism of a dental glass-ceramic. *Wear*, 1995, **181-183**, 821–825.
16. Cai, H., Marion, A., Kalceff, S. and Lawn, B. R., Deformation and fracture of mica containing glass-ceramics in Hertzian contacts. *Journal of Materials Research*, 1994, **9**, 762–770.
17. Yu, H. Y., Cai, Z. B., Ren, P. D., Zhu, M. H. and Zhou, Z. R., Friction and wear behavior of dental feldspathic porcelain. *Wear*, 2006, **261**, 611–621.
18. Zhum, G. K. H. and Neumann, P., Oscillating sliding wear of cordierite glass and ceramic in liquid media. *Wear*, 1997, **203–204**, 107–118.
19. Nagarajan, V. S. and Jahanmir, S., The relationship between microstructure and wear of mica-containing glass-ceramics. *Wear*, 1996, **200**, 176–185.
20. Nagarajan, V. S., Jahanmir, S. and Thompson, V. P., In vitro contact wear of dental composites. *Dental Materials*, 2004, **20**, 63–71.
21. Roy, S. and Basu, B., On the development of two characteristically different crystal morphology in SiO_2–MgO–Al_2O_3–K_2O–B_2O_3–F glass-ceramic system. *Journal of Materials Science: Materials in Medicine*, 2008, **20**(1), 51–66.
22. Roy, S. and Basu, B., In vitro dissolution behaviour of SiO_2–MgO–Al_2O_3–K_2O–B_2O_3–F glass-ceramic system. *Journal of Materials Science: Materials in Medicine*, 2008, **19**, 3123–3133.
23. (a) Molla, A. R. and Basu, B., Microstructure, mechanical, and in vitro properties of mica glass-ceramics with varying fluorine content. *Journal of Materials Science: Materials in Medicine*, 2009, **20**, 869–882;
(b) Molla, A. R., Influence of ceramising treatment on the crystal shape, in vitro and tribological properties of machinable glass ceramics; M. Tech thesis, IIT Kanpur, July 2007.
24. Kumar, B. V. M. and Basu, B., Fretting wear properties of TiCN–Ni cermets: influence of load and secondary carbide addition. *Metallurgical and Materials Transactions A*, 2008, **39**, 539–550.
25. Li, H. and Zhou, Z. R., Wear behaviour of human teeth in dry and artificial saliva conditions. *Wear*, 2002, **249**, 980–984.
26. Klaffke, D., Fretting wear of ceramics. *Tribology International*, 1989, **22**, 89–101.
27. Sarkar, D., Basu, B., Chu, M. C. and Cho, S. J., Is glass infiltration beneficial to improve fretting wear properties for alumina? *Journal of the American Ceramic Society*, 2007, **90**, 523–532.
28. Karanjai, M., Kumar, B. V. M. and Basu, B., Fretting wear study on Ti–Ca–P biocomposites in dry and simulated body fluid. *Materials Science and Engineering A*, 2008, **475**, 299–307.
29. Johnson, K. L., *Contact Mechanics*. Cambridge University press, UK, 2001, pp. 93.
30. Archard, J. F., Contact and rubbing of flat surfaces. *Journal of Applied Physics*, 1953, **24**, 981–988.